MOTION: MAV Operated Tunnel Inspection using Object-classification Neural Networks

Christian Burwell
Northeastern University
Boston, Massachusetts
burwell.c@northeastern.edu

Tianqi Huang
Northeastern University
Boston, Massachusetts
huang.tian@northeastern.edu

Rohit Pal
Northeastern University
Boston, Massachusetts
pal.r@northeastern.edu

Michael Shen
Northeastern University
Boston, Massachusetts
shen.mich@northeastern.edu

Harrison Sun
Northeastern University
Boston, Massachusetts
sun.har@northeastern.edu

Eagle Yuan
Northeastern University
Boston, Massachusetts
yuan.e@northeastern.edu

Taskin Padir
Northeastern University
Boston, Massachusetts
t.padir@northeastern.edu

Bahram Shafai
Northeastern University
Boston, Massachusetts
shafai@ece.neu.edu

***Abstract*—Recent infrastructure collapses, such as the MBTA's Government Center collapse, have highlighted the importance of safe and efficient methods for evaluating critical infrastructure. To combat this issue, we have developed a small Unmanned Aerial System that can detect and evaluate the risks associated with hazardous fractures within tunnel walls. In our proposed solution we are leveraging Region-based Convolutional Neural Networks (R-CNN) for an applied mask in computer vision, Simultaneous Localization And Mapping (SLAM) for global navigation in GPS-denied tunnels, and an integrated sensor suite for visualizing and interpreting crack integrity while maintaining flight capabilities in remote environments. With these techniques, we have the capability to deploy a tool that provides insightful analysis of various civil infrastructure evaluations to expert civil engineers. With the developed system we hope to provide the industrial and academic communities with a prototyped system that can help mitigate the impact of cracks in vulnerable infrastructure.**

I. Introduction

The recent collapse of the Government Center, as well as consistent MBTA closures within Boston have proved the local shortcomings with infrastructure [1]–[3]. Additional collapses such as the Surfside condo collapse in Florida have demonstrated how devastating human oversight can be when infrastructure issues are ignored [4]. The White House in particular has made it clear that this is an integral issue with their proposed Build Back Better plan, which aims to rebuild existing American infrastructure such as bridges and roads [5]. In a study conducted by Friswell MI and Penny JET, it was found that cracks are one of the best visual indicators of structural damage [6]. Cracks in the foundations of the buildings were some of the main causes of the Surfside condo collapse [7]. Current tunnel designs make it difficult to safely inspect the damage to the infrastructure [8]. Researchers have been experimenting with the idea of sending engineering-designed solutions in place of civil engineers to evaluate tunnel infrastructure to expand the accruable set of data and ensure the safety of engineers and workers.

This can be seen with the usage of UAVs in Boston's MBTA system, where MassDOT deployed a human-operated UAV within the Green Line's tunnel system to safely assess conditions following the government center collapse [9]. Additionally, Amberg Technologies and Engineering from Switzerland have explored the use of autonomous robots and cars within tunnels with their Mobile Infrastructure Scanning System [10].

The use of drones has allowed workers to examine the current conditions of civil infrastructures without needlessly putting lives at risk. However, the level of detail currently being collected through the use of UAVs is limited. On the other hand, existing robots are limited in their mobility and ability to access confined spaces.

This capstone project further expands upon existing solutions by leveraging UAVs to curate an extensive and detailed set of data. This data can then be used by civil engineers to properly analyze the risk. This capstone project specifically examines the capabilities of UAVs to autonomously identify and collect data on surface as well as subsurface cracks.

II. Background

A. Hazardous Environments

One of the prevalent issues in the environments where infrastructure lies is the safety of workers. Specifically, in tunnels, there are concerns about collapses and floods, and leaks. As mentioned earlier, there was a concern for a potential collapse of the tunnel system after the Government Center collapse in Boston's MBTA system, prompting an inspection with a human-operated UAV by MassDOT [9].

Another safety concern is the potential for toxic fumes and dust that trickle through tunnel systems, as well as other

infrastructures where ventilation is a consideration of the design [11]. This is particularly a concern for workers and travelers who get exposed to these unsafe conditions, which could cause serious lung issues.

There is also a concern about the physical location of the infrastructure. In general, some infrastructure can be hazardous in terms of the ability to get a solid vantage point for inspection. One example includes bridges, where it becomes difficult to navigate around the bridge to get vantage points to view the structural integrity of the bridge [12].

B. Infrequency and Length of Inspections

The frequency of inspections of infrastructure is dependent on the number of resources available [13]. Since these inspections can be costly to an already limited amount of resources, some collapses can be attributed to a lack of inspections. Following the Surfside collapse in Florida, a new law was proposed and passed that would require periodic inspections of older residential complexes [14]. Additionally, following the collapse in Florida, a national survey was conducted enquiring about the frequency of building inspections, and 20% of authorities having jurisdiction responded that they conduct periodic inspections on existing buildings [15].

These inspections of larger pieces of infrastructure do take more time compared to smaller pieces of infrastructure, especially if these inspections are not assisted. Due to the length of these inspections, extensive lane closures are required to accommodate the workers, backing up traffic along these roads [12]. In other inspections such as the MBTA system, it leads to longer suspensions of the system, which also causes backed-up traffic as more commuters look for alternative solutions of transportation. These all lead to more delays and closures, as inspectors need to move large pieces of equipment and deploy them in the infrastructure to complete the investigation.

C. Subsurface Cracks

When discussing visual examples of cracks, surface-level cracks are the ones that often come to mind. However, another important dimension to the integrity of materials is subsurface cracks. The issue arises when some of the more common methods of subsurface crack detection are destructive methods [16]. Although these methods do detect structural damage, there are drawbacks, especially just considering the destructive nature of these methods.

More recently through the assistance of technology, there are more nondestructive methods to detect these subsurface cracks. Techniques such as using ultrasonic and radiography have made subsurface crack detection easier [17]. However, these techniques also have drawbacks, as they do require more technical maintenance and expertise to conduct and understand these inspections. Additionally, radiography is considered dangerous due to the implementation of ionizing radiation and its effects on humans exposed to it [18].

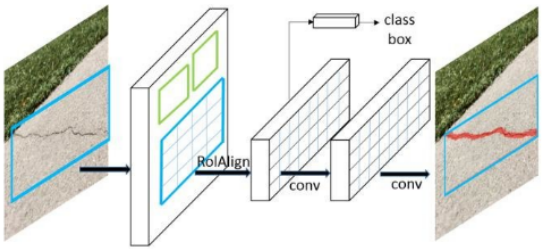

Fig. 1: Overview of Mask R-CNN

III. Methodology

A. Mask-RCNN Computer Vision

Mask R-CNN is an instance segmentation technique that can detect multiple objects in each frame [19]. This technique allows accurate detection of object location and boundaries, even when there are multiple instances of the object in the same image. The object data is stored using pixel coordinate data and can be displayed graphically to the end user. As shown in Figure 1, this can be used to highlight areas of concern for closer inspection by a civil engineer [20].

The Mask R-CNN model was trained using labeled data curated by Virginia Tech and the National Science Foundation in their "Concrete Crack Conglomerate Dataset" [21]. By utilizing a large set of labeled data, different types of surface-level crack formations in various concrete media were accounted for. This also prevented the overfitting of image mask data [22]. Furthermore, using this dataset allowed confidence in the accuracy of the dataset and focus on the model and design implementation. To further refine the model, transfer learning was applied from the COCO Mask R-CNN model for better detection of background features [23].

The model was trained on the Microsoft Azure and Google CoLab platforms [24], [25]. The cloud platforms allowed the simultaneous utilization of computational resources in a virtual environment from multiple devices. Additionally, the Azure API allows streaming image and video data and processing the data using server-side resources.

B. UAV System

The UAV, shown in Figure 2, was borrowed from Northeastern University's UAV club (NUAV) to act as a stable research platform for the project. The UAV, henceforth called the FROG, is a 14" propeller-class quadcopter running PX4 flight software. Onboard it is equipped with a Jetson Nano mission computer and a Realsense D435i RGB-D camera for navigation. The FROG has been utilized by NUAV for research and has proven itself as a versatile UAV research platform. On top of the base FROG, we added a T265 tracking camera to handle GPS-denied localization as well as an array of high-powered LEDs to provide light in dark tunnels. The high-level system diagram is shown in Figure 3.

1) Simulation: To develop autonomous capabilities for the proposed UAV, a suite of simulation software was utilized. This suite consisted of a firmware simulation provided by

Fig. 2: Aerospace NU NUAV Frog Drone

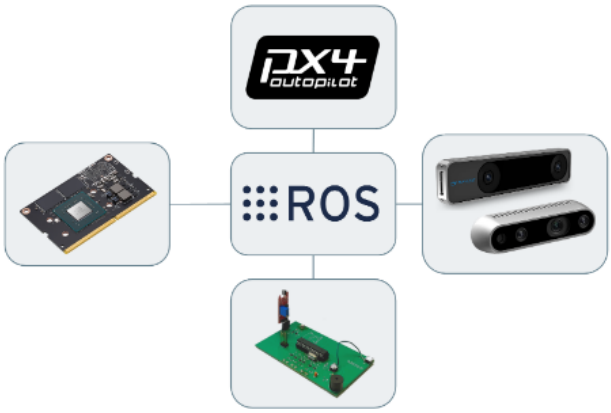

Fig. 3: High-Level System Diagram

PX4, along with the Gazebo physics simulation environment as shown below in Figure 4. By testing in simulation, code and algorithms could be developed quicker and verified without any risk to hardware or personnel. In particular, this allowed us to develop a Visual-Inertial Odometry driver before testing it in hardware later.

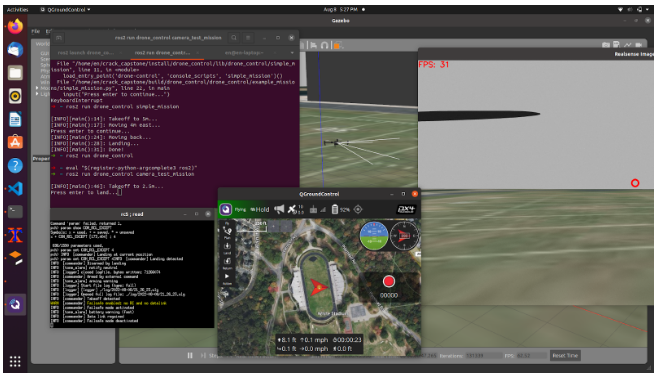

Fig. 4: Gazebo Simulation Environment

2) Px4: PX4 is an open-source autopilot designed to be used in a wide range of use cases from consumer drones to industrial applications. It is also the leading research platform for drones across the world. In this project, PX4 provided the UAV with its core control and safety features. This allowed the focus to be shifted to higher-level problems such as route localization in GPS-denied environments. PX4 was able to be controlled via MAVLINK, and provided the ability for external odometry input. This allows us to integrate our Visual-Inertial Odometry driver with ease.

3) Visual Inertial Odomoetry: As previously mentioned, the UAV needed to navigate through tunnels which are often GPS-denied environments. As most drones rely on GPS, including the FROG provided by NUAV, another navigation method was needed. One such solution was visual-inertial odometry which combines inertial measurements from the UAVs IMU with odometry information from a visual navigation sensor or algorithm. Through connection with Northeastern's Robotics Club, we were able to obtain a T265 Tracking camera which could provide us with the visual components needed. With the aid of a custom driver, we were able to relay the T265's odometry data to PX4, providing it with another source of information to localize itself within the tunnel.

C. Simultaneous Localization and Mapping

One of the issues with flying a drone within a tunnel is the fact that it is a GPS-denied environment. Another way in which we tackled this issue was by leveraging a novel algorithm called Simultaneous Localization & Mapping. This allowed us to autonomously navigate our UAV through a tunnel system. We used two implementations of this algorithm: STELLA ORB V2 and RTAB Map. These implementations of SLAM could efficiently and accurately generate 2D as well as 3D maps. Our UAV used these maps for fast, efficient localization.

1) STELLA ORB V2: One of the first implementations of SLAM that we explored was called STELLA ORB V2. The novelty of this algorithm was its ability to generate highly accurate 3D maps. STELLA has the capability to leverage both mapping and localization for its first phase of generating maps and can then utilize the generated maps for efficient, accurate localization. STELLA does the mapping and localization phase with a series of features and landmarks as seen in Figure 5 in order to determine the location of the drone for mapping. Features are points identified within an image that has a degree of variances such as a crack in a wall, a corner, or the edge of a table. STELLA is consistently evaluating all of the features within the images that are fed in through a realsense camera. Landmarks are simply features that have been established to have a certain degree of confidence across several frames. The generated map is a mathematical binary file that includes the locations of all of the landmarks that were deemed to have proficient confidence.

2) RTAB MAP SLAM: Apart from STELLA SLAM we explored another form of SLAM called RTAB MAP SLAM. The main difference between STELLA and RTAB is that:

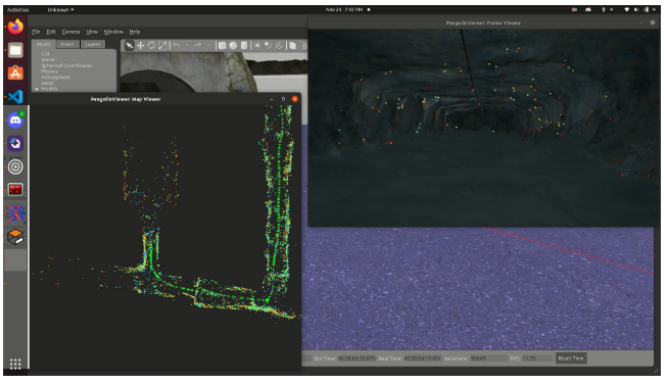

Fig. 5: Features are represented by all of the points within the image and landmarks are identified as features that are closer to the color green

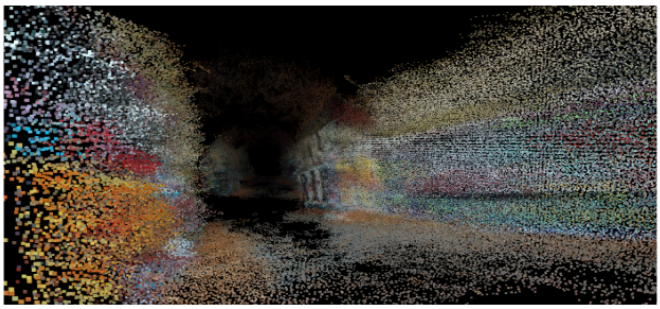

Fig. 6: Point Cloud Map generated by RTAB MAP SLAM

- RTAB generated 2D maps for localization as opposed to 3D maps
- RTAB creates much nicer and more detailed point cloud maps that a user could more easily interpret. These maps are however not used for localization and are used purely from a visual perspective

As opposed to using a system of features and landmarks like STELLA does, RTAB MAP SLAM just takes in point clouds of information and keeps all the information that appears to align from frame to frame.

This resulted in more visually appealing maps that were great for visual interpretations of our tunnel infrastructures (as seen below in Figure 6). This allowed us to verify, to an extent, the capabilities of this implementation of SLAM. One of the issues with RTAB is that it requires high-light environments in order to function effectively.

D. Sensor Suite

1) On Board LEDs - Front Light System: LEDs are fundamental for ensuring the safe operation of the drone. These LEDs act as an indicator for oncoming workers to show that the drone is operational and that caution should be exercised. Furthermore, LEDs provide directional lighting for when the UAV is operating in dimly lit conditions. These LEDs act as a reliable light source for the RGB-D camera to highlight cracks,

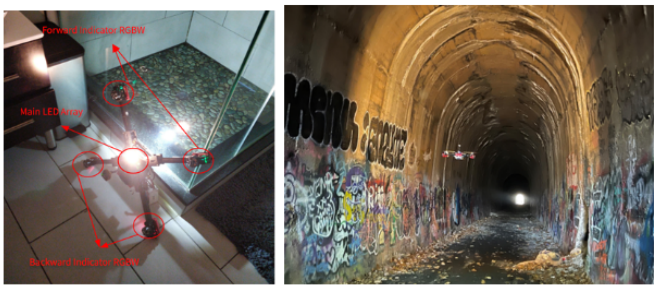

Fig. 7: On-board LED system demo

which would otherwise not be detected visually. This concept is illustrated in Figure 7 [26].

To support our visual sensors (RGB camera), an LED front light system was integrated on the board, and the system was designed to support the full functionality of cameras working in a low-light environment. In more detail, the design rules of the system were: economic, low power dissipated, and universal to all other drone platforms.

The LED system should be budget-saving, not only reduced in the design stage but also should be cheap in the production stage as well. Therefore, the prototype of the system was designed based on LED light bulbs. Our team did experiments on removing the voltage converter set up inside each stock product, and generally, a 6-set of LED lights has an average market price of $10, and the total cost added extra aftermarket modifications, including wiring, power adapting, and physical mounting would be about $15 for each system.

Meanwhile, to maximize the entire task hours of the drone, the front light should minimize power consumption as much as possible. A current driver was set up to power the diodes with current controls, and that allowed the device to be suitable for different demands of illumination. According to our most recent test shown in Figure 8, we powered the system with 0.05 Amp, and the system did reach a suitable illumination in Clinton Tunnel. The illumination level was reliable to the cameras on smartphones and human eyes. Nevertheless, our team learned that our RealSense device required more exposures on the pixels, to generate clear image captures.

By the end, the 3D printed stand was designed based on the mechanical schematic of the drone by SolidWorks, and the designing and printing process should be repeated easily on all other drone platforms.

2) On Board LEDs - RGBW Indicators: There was another colorful LED system targeting operating safety, which includes 4 independent RGBW (red, green, blue, and white) units under all 4 of the propellers. The RGBW units had the same expectations as the front-light systems. Each unit cost less than $4, and it ran at 5mW for each unit; Meanwhile, there were 4 MOSFETs controlling 4 different channels, and the user should be able to program the RGBW devices easily with GPIO connection (3.3 5V); Therefore, the RGBW indicators were fully programmable for different demands from users, and the users could script different light signals depending on

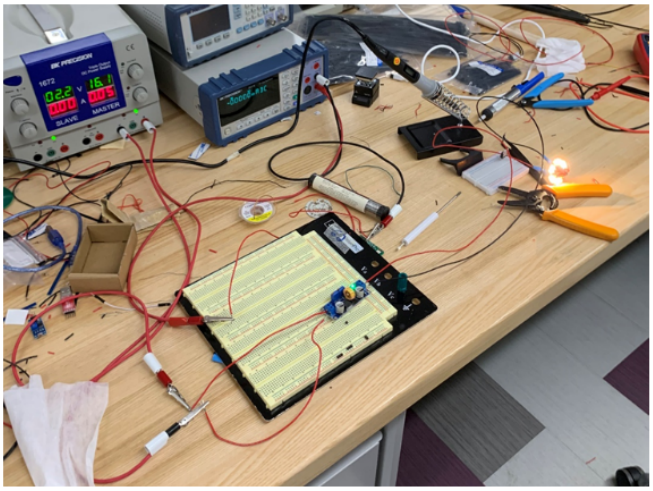

Fig. 8: Front light unit in bench tests

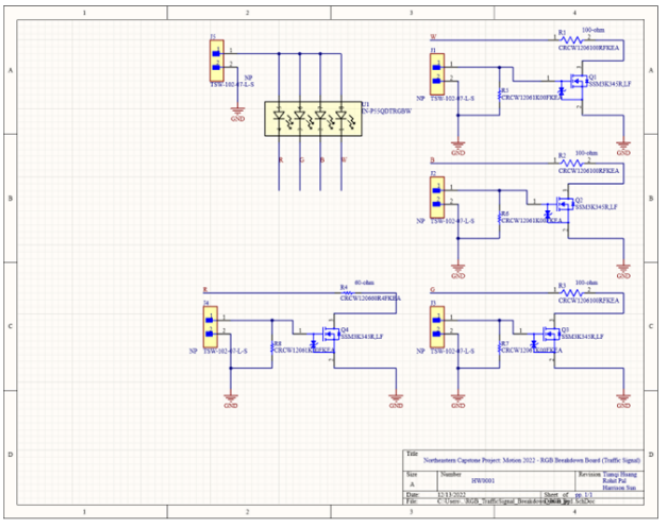

Fig. 9: The schematic of the RGBW indicator

their requirements.

3) Hall Effect Sensor: Another hardware component that was integrated into our drone was the Hall Effect Sensor suite. A Hall effect sensor detects the magnitude of a magnetic field based on its field strength. The primary purpose for using such a sensor was to create a proxy for subsurface crack detection. This Hall Effect Sensor suite was created from the ground up. It used the ATMEGA328p microcontroller and connected to several indicator LEDs and a buzzer. Furthermore, the hall effect sensor was being used as a peripheral. The six LEDs were each separated into mild, medium, and high magnetic field indicators.

We tested this concept by embedding magnets in styrofoam. These magnets were embedded at different distances from the sensor. Each time the hall effect sensor would detect a magnetic field, its corresponding LEDs would light up along with a high-frequency buzzer tone. As the hall effect sensor

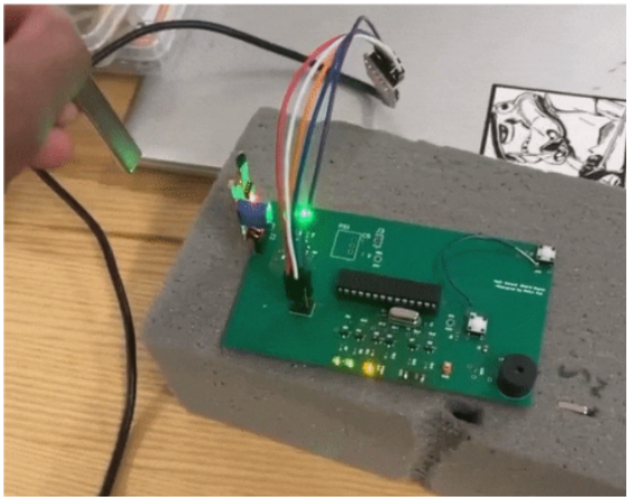

Fig. 10: Hall Effect Sensor Demo

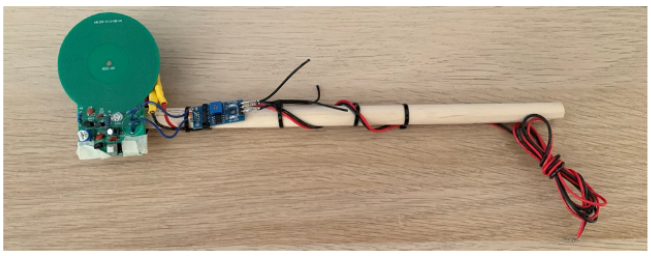

Fig. 11: A Proxy of the Metal Detector Add-on Unit

detected the magnetic field closer to proximity, the buzzer frequency would increase and different indicators would light up. The figure below highlights the hall effect sensor in action, without the use of styrofoam. This hall effect sensor suite was also attached to the drone by using the drone's 24V battery and bucking it down to 5V.

E. Metal Detector Sensor

Besides the hall effect sensor suite, there was one more device, which was also targeting subsurface detection proxy, which was under bench tests. A metal detector was crafted by market-existing products with an inductor pad and a comparator built-in photoresistor Arduino kit, and the device was designed to detect all different metals through air median and should be easy to connect with a motherboard with GPIO for data transmission, this can be seen in Figure 11. However, the device was equipped on the drone, due to a lack of detection abilities through solid medians, like concrete, and requires multiple noise-less DC supplies which were not available on our current testing drone.

IV. Results

A. Integration Tests

We conducted two main integration tests to validate the functionality of our system. Our first test was conducted at Franklin Park in Boston, Massachusetts, and our second

Fig. 12: Integration Test of System in the Miniature Franklin Park Tunnel

Fig. 13: Full Integration Test of System in the Clinton Tunnel

test was conducted at the Clinton Tunnel in Clinton, Massachusetts. Both these tests were similar in making sure all of the components of our onboard system were working correctly.

The Franklin Park test served as a preliminary investigation into our system. We were able to test flight software and more importantly fly with an implementation of a SLAM algorithm onboard. We were able to conduct an autonomous drone test with SLAM in a miniature tunnel at Franklin Park, building up to a full-sized tunnel.

After we validated our system in a miniature tunnel, we shifted to testing at a full blown tunnel. Here, we tested that we could use the additional hardware lighting we integrated into the drone, used SLAM in a flight test of the drone in the tunnel, and tested our subsurface proxy sensor of the hall effect sensor. We then tested our computer vision algorithm offboard based on the data we collected from the Clinton tunnel test.

Both these tests were a tremendous success, where we were able to pass all of our integration goals. The following sections go further into the individual components that make up our whole system, including their initial testing and specific final testing results.

B. SLAM Tests

Through our testing we found that we needed to modify the way we used STELLA SLAM in order to ensure that hardware on board the drone could handle the computing necessary for it. When testing STELLA within an actual tunnel system we observed two things:

- Mapping was more compute-intensive compared to localization
- Running STELLA with RGB was also more compute-intensive when compared to when running STELLA with infrared depth data

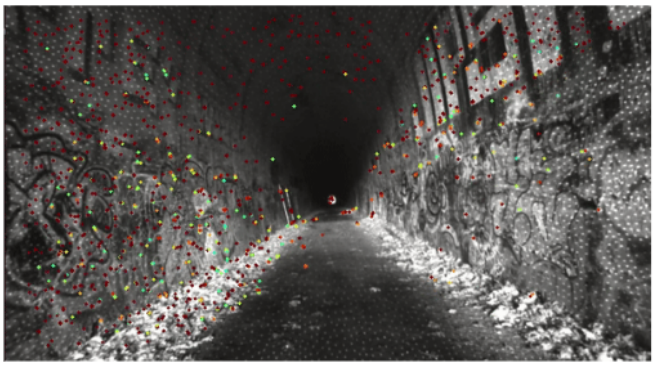

Fig. 14: STELLA ORB V2 SLAM implementation using depth data instead of RGB data

Given the limited computational power available on our drone it was important that we limit the computing if we wanted to pull off accurate and efficient mapping and localization. The first thing we did was lower the compute from input data by simply providing infrared depth data instead of RGB data. This didn't result in any significant loss of information. However, with mapping, it was still computationally very intensive and unavoidable due to it being an integral part of our SLAM implementation. We approached this by separating the mapping and localization phase entirely. Mapping was handled manually on other hardware that could use the computing necessary to run mapping and our UAV handling the less intensive localization for tunnel inspection using the maps generated

C. Computer Vision Tests

After training our model on the Virginia Tech Crack Dataset and applying transfer learning from the COCO model, we tested against a curated validation dataset. We achieved a validation accuracy of 96% as compared to an 82.9% human labelling accuracy as found in the literature [27].

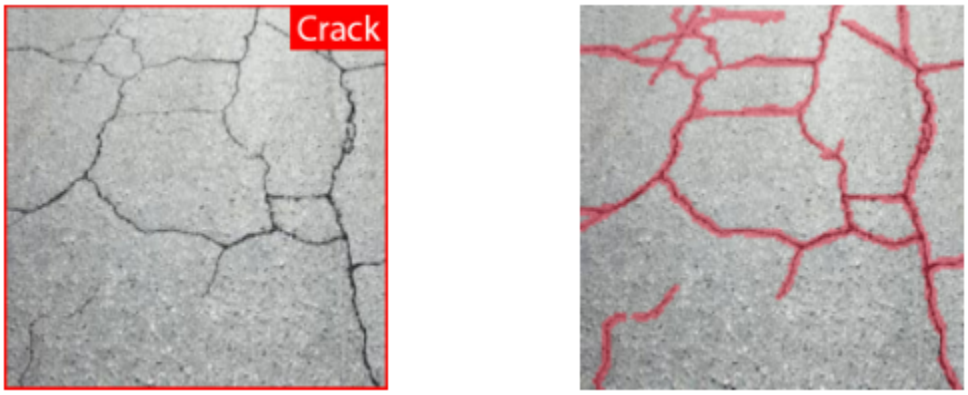

Fig. 15: Computer Vision model comparison of bounding boxes (left) and MASK R-CNN image segmentation (right)

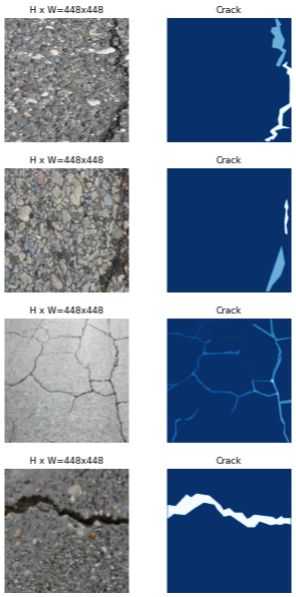

Fig. 16: Generated Masks from Mask R-CNN

As seen above in Figure 15, we were able to successfully implement image segmentation (right), which resulted in pixels being individually labeled to indicate which pixels resulted in the classification. This provides higher explainability for the model and bolsters confidence in the results when compared to standard bounding box techniques (left) [28].

As seen in Figure Figure 16, an additional benefit of this technique is that the masks are also output as a mask file, which shows the cracks on a solid color background. Different instances are shown in different colors and the cracks are easily distinguishable from the background features. This allows civil engineers to easily process large amounts of video data without the distraction of tunnel features and the related exhaustion that comes with it.

D. Simulation Tests

In order to sanity test the capabilities of our software we leveraged a modern and advanced simulation engine called Gazebo in order to test the capabilities of our software systems before applying them to hardware.

One of these tests we conducted within simulation was the verification of STELLA ORB V2 SLAM. To approach this we designed a simulation world that mimicked the conditions of Edgar Tunnel in Colorado and ran our simulated UAV through the system with STELLA implemented on it through it. Through this test we discovered some of the limits of this implementation of SLAM within a tunnel environment.

- An inversion of red and blue colors
- The speed at which the UAV could travel without losing SLAM mapping was limited to approximately 2-3 mph

However, despite these limitations we found that SLAM within a simulated environment was capable (under ideal conditions) of generating highly accurate maps for autonomous navigation.

E. Hardware Tests

According to our last flight test in the Clinton Tunnel, our new integrated hardware was finally tested in-field. We ran multiple tests targeting different parts of our design, and we did achieve positive feedback on our design concepts, but we also learnt more about the potential updates aiming at those unexpected conditions we could not simulate in the lab. The LED system was working at our expectation, and it provided a suite light source inside the tunnel. We have found that we need to increase the power of our LED system in order to better match the power required for the RealSense camera to produce clear pixels. At the same time, we have also realized that the IR camera performs well in tunnels, so we have also considered the possibility of using the IR camera from a hardware and software standpoint. In general, we will enhance our hardware optimization for low-light usage environments in order to make our design excel in future applications.

We further tested the Hall effect sensor in the Clinton Tunnel. This was done embedding magnets into the wall through tape and maneuvering the drone in close proximity. The buck converter that was being utilized by the hall effect sensor suite worked flawlessly as the 24V drone battery was being bucked down to 5V, Significant power dissipation was

not observed as the board did not show any signs of significant temperature increase. Once the drone was brought close to the magnets, the buzzer was able change its frequency based on the strength of the field, and the indicators worked as expected. Therefore, this sensor suite was validated successfully, and the Clinton tunnel provided valuable field data. If we were to enhance this sensor suite in the future, the Hall effect sensor would have to be made much smaller. The PCB can be adjusted into an even smaller package in order to reduce weight and compactibility when attached to the drone.

V. Future Work

A. Sensor Suite Expansion

1) IR Thermal Camera: Infrared thermography is another non-destructive technique that can be used for crack detection. An IR thermal camera and a thermal heat source can be used to produce a live thermal picture of a crack based on the thermal radiation emitted from it [29]. In order for infrared thermography to properly function after the application of the thermal pulse, the temperature of the defect must change rapidly after the initial offset since thermal energy propagates through diffusion. The slope of the temperature differential can be calculated from the thermal sensor in order for the crack to be determined [30].

2) RGB-D Camera: An RGB-D camera can be used for image-based crack detection and may provide insight into the crack's depth [31]. The addition of depth on top of the RGB can help to identify the 3D characteristics of the crack. This data can be used to build out a more representative 3D model of the surface defects. Furthermore, the depth data can be used for the navigation of the UAV.

3) Ground Penetrating Radar: Ground Penetrating Radars (GPR) have had a demonstrated use for locating buried structures, finding utilities, and studying subsurface features. Our sensor suite would benefit from further investigation of the use cases that GPRs could have and whether they can be used for detecting cracks. According to a short description from Professor Jeffrey Daniels at Ohio State University, "under favorable conditions, GPR can provide precise information concerning the nature of buried objects" [32]. GPR was initially developed as a penetrating detection method for understanding those 'buried' and 'unseen' objects or structures underground.

"GPR has had a certain tradition in the field of diagnostics of transport infrastructure structures. GPR is usually not used as an acceptance test of new structures, but rather for the identification of weak and damaged parts of a structure, which occur within its use" [33]. Nowadays, with the development of GPR, it has been widely used to inspect not only underground but also for infrastructures by its extraordinary penetrating capability. In place of our proxy hall effect sensor, future work would be to integrate GPR into the location of our hall effect sensor to detect near-surface cracks, which will provide a new dimension of data for the inspectors about what is happening and what will happen with the inspected infrastructure.

As GPR may be difficult to obtain, Professor Carey Rappaport, an expert in sub-surface imaging, suggested the use of

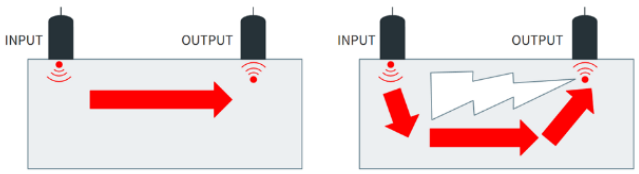

Fig. 17: Fundamental Idea of Ultrasound Detectors. Fine piece (on left) and damaged piece (on right)

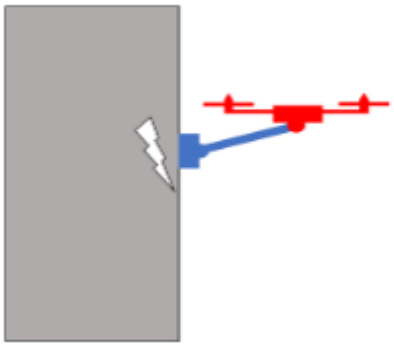

Fig. 18: Detecting subsurface cracks. MAV (in red). Contacted detection add-on (in blue)

ultrasonic transducers, which we could integrate into our proxy instead. Such a system would attach an ultrasonic speaker and microphone to the object being observed. This would provide the input and output of the signal propagating inside the object. Fractures in the material should result in changes in signal level and phase, as shown in Figure 17.

In the current stage, it is planned to focus on the signal attenuation and phase difference during the signal traveling through the object. However, it is yet to be decided which one would be of main concern before more experiments are made in practice.

In addition, there are some running equipments that are working with the same concept right now. Ultrasonic Pulse Velocity (UPV) has been deployed as non-destructive testing for quality inspection which focuses on the propagation speed inside the concrete [34]. The engineer would compare the traveling speeds past different concrete objects, and this detection method is actually a practical implementation focusing on a phase difference approach.

Figure 18 shows an abstracted image of the plan to implement the contact detection method with the UAV. Implementing this method would require a complex algorithm to simultaneously handle flight control and sensor contact. Since such an algorithm would require considerable design time, the contacted method is considered an optimal solution that will be implemented if time permits.

B. Data Pipelining

During the inspection phase of the system, we generate quite a lot of data, ranging from videos during flight to drone

readings such as altitude. Our main post-processing of data is to run our computer vision algorithm for crack detection on the video. Our model is quite computationally intensive, and it becomes difficult to port from a drone to a local machine. Instead, it would be nice to integrate post-processing of the video and run the model on the video through a cloud service. This would also allow us to utilize the cloud service's other tools to deploy a better visualization of the output of all our information including the model's output and allow civil engineers to utilize this tool with all the data. Additionally, due to the large amount of data we collect, this provides a convenient method to store our data in the cloud.

This visualization tool could include the post-processed video and a representation of where the video is in the SLAM map. This is actually really useful to civil engineers, as this is a great way to triangulate exactly where the crack detected from the computer vision algorithm is in the real environment. Additionally, we can visualize the readings of our subsurface crack detection mechanism, so that civil engineers can get an idea of also where the subsurface cracks are within the environment.

VI. Conclusion

In this paper a project we aimed to improve upon the current techniques for safely evaluating tunnel infrastructure. We leveraged a UAV and techniques such as Mask R-CNNs, an advanced sensor suite as well as SLAM algorithms for navigation and analysis within GPS-denied tunnels. Ultimately, we have proved the feasibility of sub-surface crack inspection within dark dimly lit GPS-denied tunnel environments. This work will hopefully be used in the future to further develop safe methodologies for infrastructure integrity evaluation.

VII. Acknowledgements

The authors of this paper would like to thank: Professor Bahram Shafai and Professor Taskin Padir for their support throughout this project; Frannie Hodge and Dean Briggs from Massachusetts Greenway Trust Association for their time and support throughout our integration test at Clinton Tunnel in MA; All of our peers who listened to our presentation and supported us throughout the semesters of work.

References

[1] "Spill the T: How bad is the Green Line disruption from the Government Center garage collapse?," News, Apr. 04, 2022. https://www.wgbh.org/news/local-news/2022/04/04/spill-the-t-how-bad-is-the-green-line-disruption-from-the-government-center-garage-collapse (accessed Aug. 23, 2022).

[2] "Deadly Boston Parking Garage Collapse: Here's What We Know," NBC Boston. https://www.nbcboston.com/news/local/deadly-boston-parking-garage-collapse-what-we-know/2681759/ (accessed Aug. 23, 2022).

[3] "MBTA will shut down Green Line service from downtown Boston to Somerville for nearly a month." https://www.wbur.org/news/2022/08/05/green-line-government-center-union-extension (accessed Aug. 23, 2022).

[4] X. Lu et al., "A preliminary analysis and discussion of the condominium building collapse in surfside, Florida, US, June 24, 2021," Front. Struct. Civ. Eng., vol. 15, no. 5, pp. 1097–1110, Oct. 2021, doi: 10.1007/s11709-021-0766-0.

[5] "The Build Back Better Framework," The White House. https://www.whitehouse.gov/build-back-better/ (accessed Aug. 23, 2022).

[6] "Crack Modeling for Structural Health Monitoring - M. I. Friswell, J. E. T. Penny, 2002." https://journals.sagepub.com/doi/10.1177/1475921702001002002 (accessed Aug. 23, 2022).

[7] "Florida's Condo Collapse Foreshadows the Concrete Crack-Up — WIRED." https://www.wired.com/story/floridas-condo-collapse-foreshadows-the-concrete-crack-up/ (accessed Aug. 23, 2022).

[8] "Tunnel Inspection - an overview — ScienceDirect Topics." https://www.sciencedirect.com/topics/engineering/tunnel-inspection (accessed Aug. 23, 2022).

[9] "MassDOT Aeronautics Division Drone Program — Mass.gov." https://www.mass.gov/massdot-aeronautics-division-drone-program (accessed Aug. 23, 2022).

[10] N. Winkler and A. Ackermann, "Value Preservation of underground infrastructure through focused conceptional planning," Amberg Eng. Ltd Switz., 2011.

[11] B. Ulvestad, M. B. Lund, B. Bakke, P. G. Djupesland, J. Kongerud, and J. Boe, "Gas and dust exposure in underground construction is associated with signs of airway inflammation," Eur. Respir. J., vol. 17, no. 3, pp. 416–421, Mar. 2001, doi: 10.1183/09031936.01.17304160.

[12] "Five Challenges for Bridge Inspections — Ohio University." https://onlinemasters.ohio.edu/blog/five-challenges-for-bridge-inspections/ (accessed Aug. 23, 2022).

[13] "STRUCTURE magazine — Bridge Inspection Frequency." https://www.structuremag.org/?p=14788 (accessed Aug. 23, 2022).

[14] M. Diamond, "Surfside a year later: What is Florida's new condo inspection law and how does it work?," The Palm Beach Post. https://www.palmbeachpost.com/story/news/2022/06/23/florida-building-collapse-surfside-year-later-what-floridas-new-condo-inspection-law/7681446001/ (accessed Aug. 23, 2022).

[15] "Overview of where we are on the existing buildings inspection issues - ICC." https://www.iccsafe.org/building-safety-journal/bsj-technical/overview-of-where-we-are-on-the-existing-buildings-inspection-issues/ (accessed Aug. 23, 2022).

[16] J. Yin, Q. Bai, and B. Zhang, "Methods for Detection of Subsurface Damage: A Review," Chin. J. Mech. Eng., vol. 31, no. 1, p. 41, May 2018, doi: 10.1186/s10033-018-0229-2.

[17] "Radiography or Ultrasonic Testing? Which One Is Better?," NDT, Sep. 13, 2019. https://www.ndt.com.au/radiography-or-ultrasonic-testing-which-one-is-better/ (accessed Aug. 23, 2022).

[18] "Radiation Hazards in the Practice of Radiology — Radiology." https://pubs.rsna.org/doi/10.1148/63.3.400 (accessed Aug. 23, 2022).

[19] K. He, G. Gkioxari, P. Dollár, and R. Girshick, "Mask R-CNN." arXiv, Jan. 24, 2018. doi: 10.48550/arXiv.1703.06870.

[20] C. Tan, N. Uddin, and Y. Mohammed, "Deep Learning-Based Crack Detection Using Mask R-CNN Technique," Aug. 2019.

[21] "Concrete Crack Conglomerate Dataset." University Libraries, Virginia Tech, Oct. 01, 2021. doi: 10.7294/16625056.v1.

[22] "An Overview of Overfitting and its Solutions - IOPscience." https://iopscience.iop.org/article/10.1088/1742-6596/1168/2/022022 (accessed Aug. 23, 2022).

[23] "matterport/Mask_RCNN: Mask R-CNN for object detection and instance segmentation on Keras and TensorFlow." https://github.com/matterport/Mask_RCNN (accessed Dec. 14, 2022).

[24] "Cloud Computing Services — Microsoft Azure." https://azure.microsoft.com/en-us/ (accessed Aug. 23, 2022).

[25] "Google Colaboratory." https://colab.research.google.com/ (accessed Dec. 14, 2022).

[26] "Inspire 1 dual searchlight mount," Drone Strobe Lights: Public Safety Drone Training Programs. (accessed Aug. 23, 2022).

[27] "Table 3 . Human Labelling: Overall accuracy: 82.9%," ResearchGate. https://www.researchgate.net/figure/Human-Labelling-Overall-accuracy-829_tbl3_29816654 (accessed Dec. 14, 2022).

[28] "Image segmentation — TensorFlow Core," TensorFlow. https://www.tensorflow.org/tutorials/images/segmentation (accessed Dec. 14, 2022).

[29] "Automated System for Crack Detection Using Infrared Thermographic Testing." https://www.ndt.net/search/docs.php3?id=8634&msgID=0&rootID=0 (accessed Aug. 23, 2022).

[30] J. Tashan and R. Al-Mahaidi, "Detection of cracks in concrete strengthened with CFRP systems using infra-red thermography," Compos. Part B Eng., vol. 64, pp. 116–125, Aug. 2014, doi: 10.1016/j.compositesb.2014.04.011.
[31] B. Wójcik, M. Żarski, M. Salamak, and J. A. Miszczak, "Extracting crack characteristics from RGB-D images," p. 2, 2021.
[32] J. Daniels, "Ground Penetrating Radar Fundamentals," Jan. 2000, doi: 10.4133/1.2921864.
[33] Civil Engineering Applications of Ground Penetrating Radar. Accessed: Aug. 23, 2022. [Online]. Available: https://link.springer.com/book/10.1007/978-3-319-04813-0
[34] FPrimeC, "Ultrasonic Testing of Concrete," FPrimeC Solutions Inc., Apr. 13, 2017. https://www.fprimec.com/ultrasonic-testing-of-concrete/ (accessed Aug. 23, 2022).